An evaluation of the $Y_2O_3:Eu^{3+}$ scintillator for application in medical x-ray detectors and image receptors

D. Cavouras[a] and I. Kandarakis
Department of Medical Instrumentation Technology, Technological Educational Institution of Athens, Ag. Spyridonos Street, Aigaleo, Athens, Greece

G. S. Panayiotakis
Department of Medical Physics, Medical School, University of Patras, 265 00 Patras, Greece

E. K. Evangelou
Physics Department, University of Ioannina, P.O. Box 1186, 45110 Ioannina, Greece

C. D. Nomicos
Department of Electronics, Technological Educational Institution of Athens, Ag. Spyridonos Street, Aigaleo, Athens, Greece

(Received 29 December 1995; accepted for publication 30 July 1996)

The suitability of a $Y_2O_3:Eu^{3+}$ scintillator for use in radiation detectors and medical image receptors was studied. $Y_2O_3:Eu^{3+}$ was used in the form of laboratory prepared screens of different coating thicknesses. The x-ray luminescence efficiency of the screens was measured for tube voltages between 50–200 kVp and in both transmission and reflection modes of observation. The intrinsic x ray to light conversion efficiency (n_c) and other parameters of the $Y_2O_3:Eu^{3+}$ phosphor material related to optical scattering, absorption, and reflection were determined. These were used in the calculation of the image transfer characteristics, MTF and zero frequency DQE, for various screen coating thicknesses and x-ray tube voltages. The light emission spectrum of $Y_2O_3:Eu^{3+}$ was measured (narrow band peak at 613 nm) and its spectral compatibility to the spectral sensitivity of several commonly employed optical photon detectors was determined. The x-ray luminescence efficiency varied with x-ray tube voltage, attaining maximum value at about 80 kVp for all screen thicknesses. It also varied with coating thickness reaching 25 $\mu W\,m^{-2}/mR\,s^{-1}$ and 18 $\mu W\,m^{-2}/mR\,s^{-1}$ at 175 mg/cm^2 for reflection and transmission modes, respectively. The intrinsic x ray to light conversion efficiency and the image transfer characteristics were found to be comparable to several commercially used phosphors: $n_c=0.095$, $MTF_{0.05}$ ranged between 10 and 25 line pairs per mm and peak values of DQE(0) varied between 0.33 and 0.14 in the coating thickness and kVp ranges useful for x-ray imaging. Spectral compatibility to some red sensitive optical photon detectors was excellent (0.9 or better). Results indicated that $Y_2O_3:Eu^{3+}$ is a medium to high overall performance material that could be used in medical x-ray detectors and image receptors.

Key words: x-ray screens, x-ray luminescence, MTF, DQE, spectral matching

I. INTRODUCTION

Scintillators in conjunction with optical detectors (films, photocathodes, photodiodes, CCD arrays) have been used as image receptors in conventional and digital radiology, and as radiation detectors in computed tomography and nuclear medicine. Yttrium oxide (Y_2O_3) is a scintillator considered suitable as a host for trivalent rare earth ion activators (i.e., Tb^{3+}, Eu^{3+}), producing sharp line emission spectra.[1] Europium doped yttrium oxide ($Y_2O_3:Eu^{3+}$ or P22) is a nonhygroscopic phosphor material, emitting reddish light with a decay time[2] around 1 ms, which is small enough for most radiological imaging applications; response times for dynamic fluoroscopic imaging are well above 1 ms due to longer TV camera lag characteristics.[3] $Y_2O_3:Eu^{3+}$ has been adopted in nonmedical applications, some of them demanding short luminescence life times, such as CRT and TV screens, scanning tubes,[4] and plasma radiation (UV and x rays) detectors.[2] However, $Y_2O_3:Eu^{3+}$ has not been widely used in medical imaging, except in x-ray detectors of CT systems.

In the present study, the suitability of the $Y_2O_3:Eu^{3+}$ phosphor material to be used in radiation detectors and/or image receptors of medical imaging systems was examined. In general, yttrium based scintillators exhibit increased x-ray detection efficiency[3,5,6] in the energy range between the yttrium K-absorption edge at 17 keV and the K-edges of other phosphors with heavier elements (e.g., 50.2 keV for $Gd_2O_2S:Tb$ and 69.5 for $CaWO_4$). Also, known yttrium based scintillators show improved x ray to light conversion efficiency with respect to the conventionally used $CaWO_4$ phosphor.[5,7,8] Additionally, europium activated scintillators exhibit very good spectral compatibility with Si photodiodes, employed in many digital imaging systems, and lower optical scattering,[9,10] due to longer light wavelengths. $Y_2O_3:Eu^{3+}$ was used in the form of laboratory prepared

 0094-2405/96/23(12)/1965/11/$10.00

screens of various coating thicknesses. The x-ray induced luminescence efficiency or absolute efficiency (AE),[9,10] the modulation transfer function (MTF), the zero spatial frequency detective quantum efficiency (DQE), and the spectral compatibility[11] to various optical photon detectors were studied. In this way, coating thicknesses, x-ray tube voltages, and screen-optical detector combinations, which provide the best performance of Y_2O_3:Eu^{3+} as radiation detector and medical image receptor, were determined. Results were compared with other high performance phosphor materials employed in commercial image detectors.

II. MATERIAL AND METHODS

Y_2O_3:Eu^{3+} was supplied in powder form with grain size of about 7 μm by Riedel de Haen-Lumilux Ltd. (Code Number 54 009). Screens were prepared by sedimentation on fused silica substrates with coating thicknesses from 20 to 240 mg/cm^2. They were excited by x rays from a Siemens Stabilipan unit with tube voltages from 50 to 200 kVp. The ability of the phosphor material to convert x rays to emitted light was determined by means of AE, defined as light flux exiting the observation side of the screen per unit of x-ray exposure rate.[9,10] The experimental setup for AE measurements has been described in detail in a previous study.[10] It comprised an EMI 9558 QB photomultiplier with an extended S-20 photocathode, coupled to a Cary 401 vibrating reed electrometer. A PTW Simplex dosimeter was employed for exposure rate measurements. Two modes of AE measurement were followed: (1) Transmission mode (front screen configuration), where light is emitted from the screen surface opposite to the incidence of the x-ray beam; and (2) reflection mode (back screen configuration), where light is emitted from the screen surface receiving the x rays. The spectral distribution of Y_2O_3:Eu^{3+} light was measured with an Oriel 7240 grating monochromator. The light spectrum was used to calculate the spectral matching factor[11] between the emitted light and the spectral sensitivity of the extended S-20 photocathode. That factor was used to correct the AE measurements.[10,11]

To assess the agreement between experiment and theory, experimentally determined AE values were fitted by formulas (see Appendix A) derived from Hamaker[12] and Ludwig[9] theoretical models. Additionally, two important parameters were determined by the fitting; the intrinsic x ray to light conversion efficiency and the reciprocal diffusion length, the latter expressing the probability of optical photon attenuation. These parameters characterize intrinsic properties that affect the performance of the phosphor material and were used in the calculation of MTF and DQE.

According to the theoretical models (see Appendix A), AE may be expressed as

$$\mathrm{AE}=f(n_c,\sigma,\beta,\rho_0,\rho_1,\mu), \tag{1}$$

where n_c is the intrinsic x ray to light conversion efficiency of the phosphor material, σ is the reciprocal of the diffusion length, and β is a parameter related to the coefficients of optical absorption and optical scattering, defined as

$$\beta=(1-R)/(1+R), \tag{2}$$

where R is the reflectivity of a thick phosphor layer with negligible light transmission through it. R was determined experimentally by reflectivity measurements following the method described by Ludwig.[9] ρ_0, ρ_1 are given by

$$\rho_i=(1-r_i)/(1+r_i),\quad i=0,1, \tag{3}$$

where r_0, r_1 are the reflectivities at the front screen surface (x-ray incidence side) and the screen-substrate interface, respectively; ρ_1 was experimentally determined by reflectivity measurements, and ρ_0 was considered to be equal to 1, because light reflection (r_0) at the front screen surface is negligible. μ is the mass attenuation coefficient of Y_2O_3:Eu^{3+}, which was calculated from data given by Storm and Israel[13] and Saloman *et al.*[14] for yttrium and oxygen.

The MTF of the Y_2O_3:Eu^{3+} screens was calculated considering each phosphor screen to be divided into a series of thin layers of thickness equal to 1 mg/cm^2. The MTF of each layer was calculated using formulas from Hamaker,[12] Ludwig,[9] and Swank,[15] employing parameters n_c and σ, determined from the fitting on AE experimental data, and parameters β, ρ_0, ρ_1, which were measured experimentally. The overall MTF was obtained by summing up each individual MTF of the consecutive phosphor layers, weighted by a relative exposure factor as described in Appendix B. MTF was determined for both transmission and reflection modes of measurement. The MTF is given by (see Appendix B)

$$\mathrm{MTF}(v)=G(v)/G(0), \tag{4}$$

where

$$G(v)=f(\tau,q,\rho_0,\rho_1,\mu,m_0). \tag{5}$$

τ is the inverse relaxation length of the phosphor material[15,16] related to σ and β by

$$\tau=\sigma/\beta. \tag{6}$$

q is related to optical parameter σ and spatial frequency v by

$$q=[\sigma^2+4\pi^2(v/d)^2]^{1/2}, \tag{7}$$

where d is the density of the phosphor material, m_0 is the mean number of optical photons created per x ray interacting in the screen, determined by the following relation:

$$m_0=n_cE/E_p, \tag{8}$$

where E is the energy of the x-ray photon and E_p is the energy of the optical photons. E_p was determined from the measured light emission spectrum of Y_2O_3:Eu^{3+}, which was found practically monochromatic with a sharp line in the red region. To confirm the accuracy of the theoretical calculations, the MTF of an 71.6 mg/cm^2 Y_2O_3:Eu^{3+} screen was experimentally determined following the square wave response function (SWRF) method.[17,18] The screen was used in combination with a red sensitive Agfa Scopix LT 2B film, usually employed in laser imagers, and a typ-53 resolution bar test pattern (2.5–100 lp/cm, Nuclear Associates, Inc., Carle Place, NY). The screen was exposed to x rays by a Phillips Medio 50 CP radiographic unit operated at 81 kVp

and 35 mAs. The bar pattern images were digitized by a MICROTEC Scanmaker II SP (24-bit color, 1200×1200 dpi) CCD scanner. Screen-film nonlinearities were corrected via the H&D characteristic curve determined by bootstrap sensitometry technique.[17] Sixty-four successive image traces transverse to the pattern bars were selected and averaged to obtain a low noise SWRF. Trace amplitudes were normalized to the image contrast at 2.5 lp/cm. MTF was calculated by Coltman's formula:

$$\mathrm{MTF}(v)=\frac{\pi}{4}\left[\frac{\mathrm{SWRF}(v)}{v}+\frac{\mathrm{SWRF}(3v)}{3v}-\frac{\mathrm{SWRF}(5v)}{5v}+\ldots\right]. \tag{9}$$

This MTF was divided by that of the CCD scanner in order to obtain the Y_2O_3:Eu^{3+} screen MTF. The MTF of the CCD scanner was determined by scanning the bar pattern alone. The radiographic film MTF was considered approximately equal to 1 for frequencies lower than 100 lp/cm.[16]

The zero spatial frequency DQE, expressing the signal to noise ratio (SNR) transfer from the input to the output of an image detector, was calculated[15,19–23] by

$$\mathrm{DQE}=A_Q A_S, \tag{10}$$

where A_Q is the x-ray quantum detection efficiency, which depends on the x-ray attenuation coefficient and on the thickness of Y_2O_3:Eu^{3+} screens, and A_S is the Swank factor (or statistical factor), describing the statistical pulse (scintillations) height distribution of optical photons emitted per x-ray photon interacting in the phosphor material. The Swank factor is given by

$$A_S=M_1^2/M_2M_0, \tag{11}$$

where M_0, M_1, M_2 are the moments of the optical pulse height distribution given by (see Appendix C)

$$M_i=f(n_c,\sigma,\tau,\rho_0,\rho_1,\mu,E_p), \quad i=0,1,2, \tag{12}$$

where n_c, σ, τ, ρ_0, ρ_1, μ, and E_p were defined in relations (2)–(8).

The spectral compatibility of Y_2O_3:Eu^{3+} light emission spectrum to the spectral sensitivities of some known optical detectors was examined by evaluating the spectral matching factor[11] by the following relation

$$a_s=\sum_{\lambda_i=\lambda_1}^{\lambda_2} S_P(\lambda_i)S_D(\lambda_i)\Big/\sum_{\lambda_i=\lambda_1}^{\lambda_2} S_D(\lambda_i), \tag{13}$$

where λ_1, λ_2 are approximately the lower (575 nm) and upper (680 nm) limits of the light spectrum (Fig. 12), $S_P(\lambda_i)$ is the normalized distribution function of the emission spectrum of Y_2O_3:Eu^{3+} measured by the monochromator, and $S_D(\lambda_i)$ is the normalized spectral sensitivity distribution function of the optical detectors. Values for $S_D(\lambda_i)$ were made available from manufacturers data (EMI, RCA, Hamamatsu, ITL, Rofin and Agfa). The detectors considered were GaAs, S-25, modified S-20, and extended S-20 photocathodes, GaAsP and extended GaAsP photocells, Si and Ge photodiodes, and Agfa Scopix LT 2B photographic emulsion.

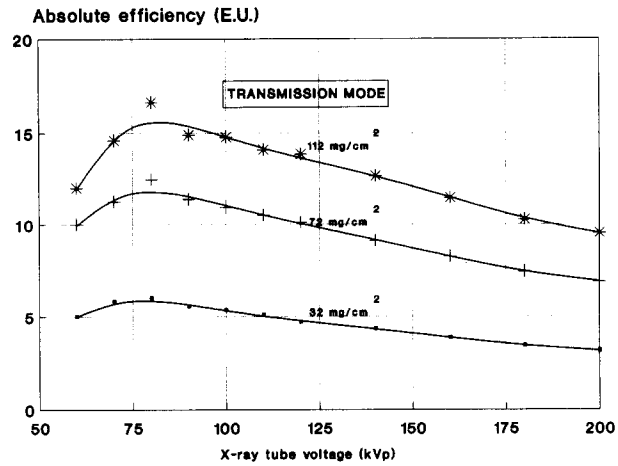

FIG. 1. Variation of x-ray absolute efficiency with tube voltage measured in transmission mode for three Y_2O_3:Eu^{3+} laboratory prepared screens of 32, 72, and 112 mg/cm^2. Points: experimental values, solid lines: theoretical curves. (1 Efficiency Unit, 1 EU=1 μW m^{-2}/mR s^{-1} or 3.875 J/C kg^{-1} m^2 S.I. units.)

III. RESULTS AND DISCUSSION

Experimental data on absolute efficiency and curves calculated according to Eq. (1) are presented in Figs. 1 and 2. AE values are given as a function of x-ray tube voltage (kVp) for three screens of coating thickness 32, 72, and 112 mg/cm^2 for transmission and reflection modes of measurement, respectively. For all screens, peak experimental values were obtained at 80 kVp in both modes. For tube voltages employed in most x-ray imaging techniques (70–80 kVp for abdominal imaging, 65–75 kVp for lumbar spine radiography, 55–65 kVp for cranial radiography, 80–120 kVp for

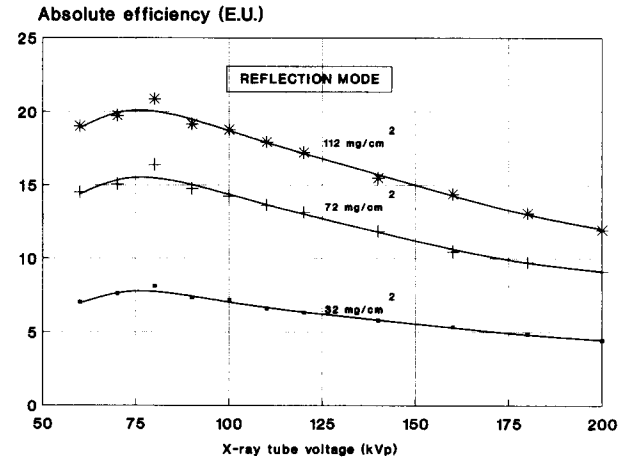

FIG. 2. Variation of x-ray absolute efficiency with tube voltage measured in reflection mode for three Y_2O_3:Eu^{3+} laboratory prepared screens of 32, 72, and 112 mg/cm^2. Points: experimental values, solid lines: theoretical curves. (1 Efficiency Unit, 1 EU=1 μW m^{-2}/mR s^{-1} or 3.875 J/C kg^{-1} m^2 S.I. units.)

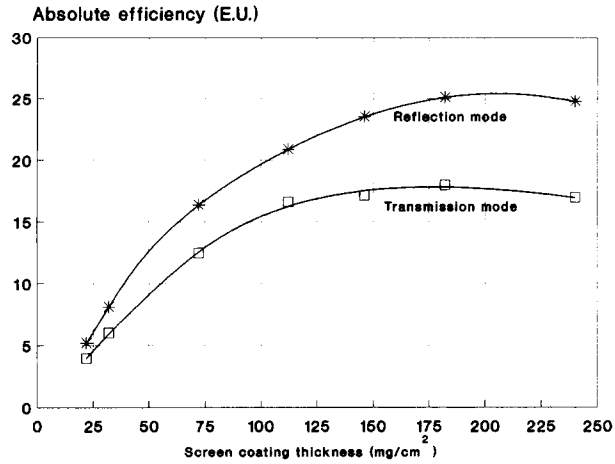

FIG. 3. Variation of x-ray absolute efficiency of $Y_2O_3:Eu^{3+}$ screens with coating thickness in transmission and reflection mode of measurement at 80 kVp. (1 Efficiency Unit, 1 EU=1 $\mu W\,m^{-2}/mR\,s^{-1}$ or 3.875 $J/C\,kg^{-1}\,m^2$ S.I. units.)

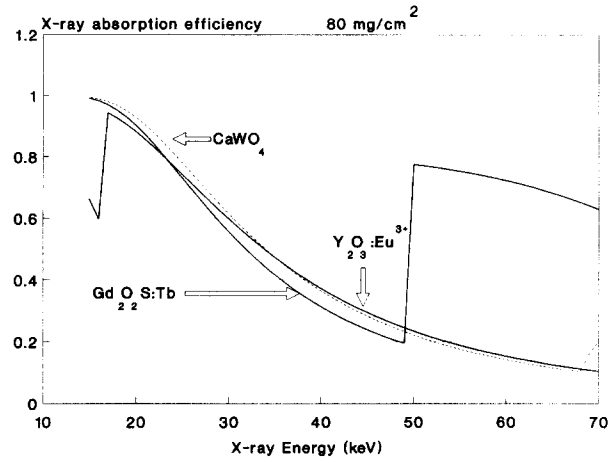

FIG. 4. Variation of absorption efficiency with x-ray energy of $Gd_2O_2S:Tb$, $CaWO_4$, and $Y_2O_3:Eu^{3+}$ 80 mg/cm^2 screens.

chest radiography, 110–120 kVp for CT imaging, 60–70 kVp for abdominal angiography) the AE values were found higher than about 75% of the peak value. Additionally, AE was better in reflection than in transmission mode and improved with screen thickness; for the screens of 112, 72, and 32 mg/cm^2 the corresponding peak AE values were 21 EU (Efficiency Unit, 1 EU=1 $\mu W\,m^{-2}/mR\,s^{-1}$ or 3.875 $J/C\,kg^{-1}\,m^2$, expressed in S.I. units), 16.5 EU, 8 EU in reflection mode and 16.6 EU, 12.5 EU, and 6 EU in transmission mode. The way that AE varies with tube voltage and screen thickness is due to the dependence of AE on x-ray absorption efficiency and light transmission efficiency through the phosphor material,[9] which in turn vary with tube voltage and depth of light photons generation, respectively.

The variation of peak AE with screen coating thickness is shown in Fig. 3. Data concerning seven screens of 20, 32, 72, 112, 148, 175, and 240 mg/cm^2 are presented for both modes of measurement at 80 kVp. Peak AE increased with coating thickness for transmission and reflection up to 175 mg/cm^2, which is an optimum coating thickness if $Y_2O_3:Eu^{3+}$ is to be used as radiation detector. As screen thickness increases, the x-ray absorption efficiency increases exponentially but light scattering and absorption effects cause a decrease in light transmission efficiency. These two competing mechanisms result in the almost flat region between 150 and 240 mg/cm^2 in the curves of Fig. 3. It is also observed that the reflection and transmission curves differ and their deviation is greater for thicker screens. This happens because light quanta mainly originate from phosphor layers near the x-ray exposed screen surface, where most x-ray quanta are absorbed. Hence, in transmission mode the distance that light quanta have to penetrate to exit the other side of the screen is longer and thus the amount of output light is smaller. It is evident that for thicker screens this effect is more intense, resulting in greater deviation between the reflection and transmission curves.

Absolute efficiency depends on the x-ray absorption efficiency, the intrinsic x-ray to light conversion efficiency, and the light transmission efficiency toward the optical detector.[9] These efficiencies are related to quantum noise because they express the ability of the phosphor material to capture primary x-ray quanta, convert them to light photons, and transmit them to the screen emitting surface. The light transmission efficiency is also related to spatial resolution because it depends on light absorption and light scattering phenomena within the phosphor material. Since noise and spatial resolution are key parameters to image quality, behavior of the $Y_2O_3:Eu^{3+}$ scintillator during those three stages of signal propagation was studied and compared with that of other phosphor materials.

Figure 4 shows the absorption efficiency, calculated as a function of energy, of three 80 mg/cm^2 screens prepared from different phosphor materials. The absorption efficiency of $Y_2O_3:Eu^{3+}$ was found better than those of $Gd_2O_2S:Tb$ and $CaWO_4$ in the ranges 23–50.2 keV (50.2 keV is the K edge of Gd) and 36–69.5 keV (K edge of W), respectively. This is due to the fact that yttrium exhibits increased x-ray absorption for a range of energies above 17 keV (K edge of Y).

By fitting theoretical models to experimental data, as shown in Figs. 1 and 2, optimum values for the intrinsic conversion efficiency (n_c=0.095) and the reciprocal of the diffusion length (σ=25 cm^2 g^{-1}) of $Y_2O^3:Eu^{3+}$ were obtained; the value of n_c is a little higher than the one previously reported[7] for $Y_2O_3:Eu^{3+}$ (n_c=0.08), which was found by cathodoluminescence efficiency measurements. Parameter β was experimentally evaluated (β=0.03) using Eq. (2), the inverse relaxation length τ was determined employing relation (6) (τ=833 cm^2/g), parameter ρ_1 was found equal to 0.818, and ρ_0 was considered equal to 1. The n_c of $Y_2O_3:Eu^{3+}$ was better or close to that of some commercially used phosphor materials, such as[5,7,8,24] $CaWO_4$ (n_c=0.035–0.05) and $BaSO_4$:Pb (n_c=0.04), employed in radiographic screens, CsI:Na (n_c=0.10), used in image intensifiers, $CdWO_4$ (n_c=0.097),[24] used in CT, and $Y_2O_2S:Eu$ (n_c=0.11), which is an yttrium compound phosphor with the same activator ion as $Y_2O_3:Eu^{3+}$. On the other hand, the n_c

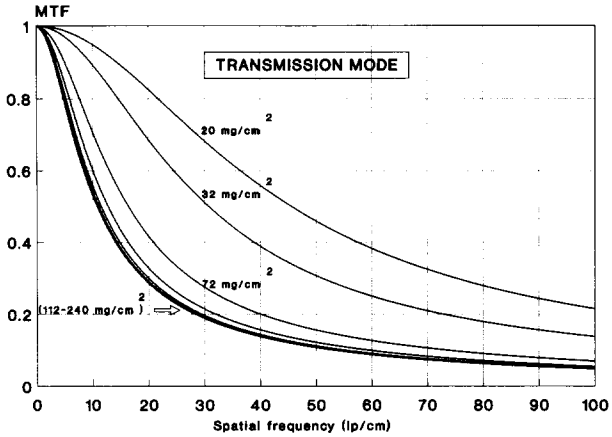

FIG. 5. Calculated MTFs of seven Y_2O_3:Eu^{3+} laboratory prepared screens in transmission mode at 80 kVp.

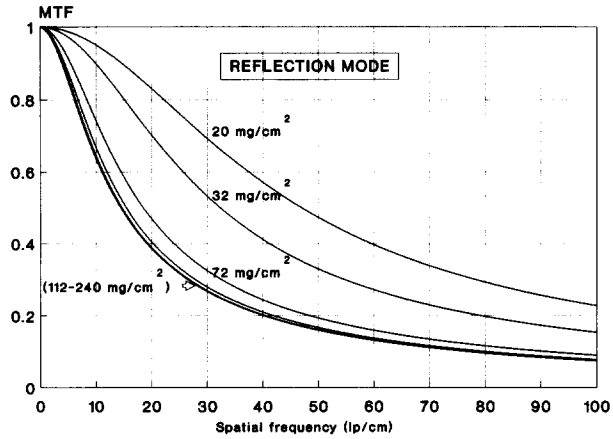

FIG. 6. Calculated MTFs of seven Y_2O_3:Eu^{3+} laboratory prepared screens in reflection mode at 80 kVp.

of Y_2O_3:Eu^{3+} was lower than that of terbium activated rare earth phosphors such as Gd_2O_2S:Tb (n_c=0.15–0.20), Y_2O_2S:Tb (n_c=0.18), and La_2O_2S:Tb (n_c=0.12–0.18).[5,7,8,25,26] Deviations in n_c among different phosphor materials may be attributed to differences in the fundamental electronic band gap of the semiconductor material,[7] the type of ion activator, the crystal structure, the site sym metry, and slightly to the size of the phosphor grains.

Optical photons transmission efficiency depends inversely on σ, which is a function of light absorption and scattering coefficients (see Appendix A). Coefficient σ was found lower than that of Gd_2O_2S:Tb (σ=30 $cm^2\,g^{-1}$), Y_2O_2S:Tb (σ=30 $cm^2\,g^{-1}$), and La_2O_2S:Tb (σ=30 $cm^2\,g^{-1}$), but higher than that of Y_2O_2S:Eu (σ=15 $cm^2\,g^{-1}$), all previously studied under the same conditions[10,25,26] with Y_2O_3:Eu^{3+}. This indicates that light attenuation is lower in Y_2O_3:Eu^{3+} than in terbium activated phosphors.

Therefore, Y_2O_3:Eu^{3+} is a scintillator material exhibiting absorption efficiency comparable to commonly used Gd_2O_2S:Tb and $CaWO_4$ phosphors for energies lower than the K edges of Gd and W, respectively, intrinsic conversion efficiency lying in between those of Gd_2O_2S:Tb and $CaWO_4$, and light transmission efficiency better than that of Gd_2O_2S:Tb. Additionally, taking into consideration that: (1) for an x-ray tube operated at 80 kVp with about 20 mm aluminum,[5] all x-ray photons are contained between 30 and 80 keV; (2) for energies between 23 and 50 keV the absorption efficiency of Y_2O_3:Eu^{3+} is better than that of Gd_2O_2S:Tb and between 36 and 69 keV is slightly better than that of $CaWO_4$; (3) the AE of Y_2O_3:Eu^{3+} attains its highest value at 80 kVp (≈55 keV); and (4) 50–120 kVp (≈30–70 keV) is the energy range used for most radiographic applications, it may be concluded that Y_2O_3:Eu^{3+} exhibits suitable physical characteristics for medical imaging applications.

Figures 5 and 6 show the calculated MTF curves for transmission and reflection modes of measurement respectively. Curves were obtained by Eq. (4) at 80 kVp, using the values found for the parameters n_c, σ, τ, ρ_0, ρ_1, and μ of Y_2O_3:Eu^{3+}. MTFs correspond to 7 screens of coating thicknesses 20, 32, 72, 112, 148, 175, and 240 mg/cm^2, which were prepared for measuring the AE of the Y_2O_3:Eu^{3+} scintillator. MTFs in reflection mode are better than in transmission mode and this is more prominent for coating thicknesses between 72 and 240 mg/cm^2. This is due to differences in the amount of light scattered and absorbed between the two modes of measurement and the phenomenon is analogous to that observed in AE measurements (Fig. 3). It is also noticed that MTF decreases with increasing coating thickness but this variation becomes smaller for thicker screens; curves corresponding to screens of 112–240 mg/cm^2 are very close, especially for spatial frequencies between 50 and 100 lp/cm (line pairs per cm).

The MTF and spatial resolution of a phosphor screen may be affected by the emission of characteristic K-fluorescent x rays. These photons are emitted by the high Z element of the phosphor material when the energy of the incoming primary x-ray photon is above the K-absorption edge (i.e., 17 keV for yttrium). A fraction of the K-fluorescent photons is reabsorbed in the phosphor material at sites different from that of primary x-ray interaction, resulting in the degradation of the screen resolution.[27,28] To estimate the importance of this effect, the ratio of the energy of $K\alpha$ and $K\beta$ x rays reabsorbed to the energy of the impinging primary x-ray photon was calculated using the analytical expressions derived by Chan and Doi.[29] This ratio was found to be 0.03 at 50 keV, which approximately corresponds to the mean energy of the 80 kVp x-ray spectrum used in the MTF calculation, and thus the K-reabsorption effect was considered insignificant.

The CCD scanner MTF, the composite scanner-screen-film MTF, the resulting experimental screen MTF, and the calculated MTF of the 71.6 mg/cm^2 Y_2O_3:Eu^{3+} screen are shown in Fig. 7. The agreement between experimental and calculated values confirms the reliability of the results. Table I shows some MTF data of a 32 mg/cm^2 Y_2O_3:Eu^{3+} laboratory prepared screen against published data[16,21,30,31] on calculated MTFs of Gd_2O_2S:Tb (Kodak Min-R) and $YTaO_4$ (Dupont Ultra-Vision) high performance commercial screens. Data were approximately estimated from published figures.

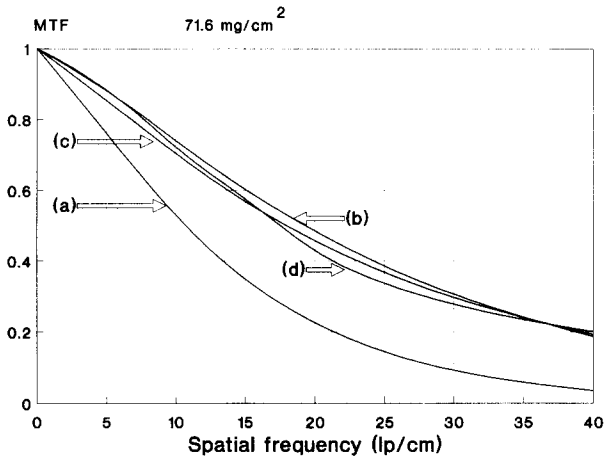

FIG. 7. Comparison of calculated and experimental MTFs of a 71.6 mg/cm^2 Y_2O_3:Eu^{3+} screen: (a) measured composite scanner-screen-film MTF; (b) CCD scanner MTF; (c) resulting experimental screen MTF; and (d) calculated screen MTF.

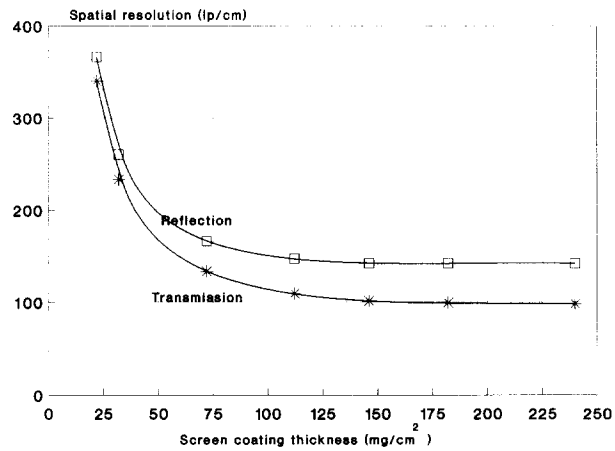

FIG. 8. Variation of the spatial resolution (spatial frequency at MTF=0.05) of Y_2O_3:Eu^{3+} laboratory prepared screens with coating thickness in both reflection and transmission modes at 80 kVp.

Figure 8 shows the variation of calculated spatial resolution (spatial frequency at MTF=0.05) with screen coating thickness. It is again observed that the resolution was better in reflection than in transmission mode, differences between the two modes were smaller for very thin screens, and degradation of resolution was minimal for screens over 112 mg/cm^2. Thus, thicker phosphor screens displaying higher AE may be used as image receptors without significant deterioration in spatial resolution. However, for thicker screens there is a more pronounced deterioration in contrast resolution in the low frequency range, as shown in Fig. 9.

Figure 10 is a plot of zero spatial frequency DQE versus coating thickness at various x-ray tube voltages, including the useful kVp range for most radiological applications. DQE was calculated using formula (10) and values of experimentally determined parameters n_c, σ, τ, ρ_0, ρ_1, E_p, and μ of Y_2O_3:Eu^{3+}; only transmission DQE values are presented because reflection mode values were not significantly different. As can be observed, each curve reached maximum at a particular coating thickness. Optimum DQE was achieved at coating thicknesses ranging between 80 and 120 mg/cm^2 for 50–200 kVp, respectively. At 80 kVp, maximum DQE (DQE=0.24) was attained at a coating thickness of 100 mg/cm^2 and DQE remained close to its highest value in the range 90–120 mg/cm^2. At higher tube voltages the peak DQE value was lower; it was shifted to higher thicknesses, but unlike low voltages, DQE values were close to peak for a wider range of thicknesses. At 120 kVp, DQE peaked between 90 and 120 mg/cm^2 (DQE=0.17) and DQE at 160 mg/cm^2 was about 91% of its peak value. Therefore, since DQE varies slowly with coating thickness at high kVp (tube voltages $\geq$120 kVp), thicker screens which are more luminescent may be employed without significant loss in SNR.

The behavior of DQE versus thickness at various tube voltages is dominated by the x-ray absorption mechanisms and the statistical pulse height distribution of emitted optical pulses, expressed by the Swank factor. As screen thickness increases, the x-ray detection efficiency (A_Q) improves causing a similar effect on DQE. On the contrary, the optical pulse height distribution broadens due to the increased amount of optical scattering and absorption on the additional phosphor grain layers of thicker screens. These effects cause greater fluctuations in the amplitudes of light pulses thus increasing noise, reducing the Swank factor, which is inversely proportional to noise,[19,20] and consequently decreas-

TABLE I. MTF data of a 32 mg/cm^2 Y_2O_3:Eu^{3+} laboratory prepared screen against calculated MTF published data of commercial screens.

Phosphor	Thickness (mg/cm^2)	Tube Volts (kVp)	Measuring mode	MTF[a] 20 cm^{-1}	50 cm^{-1}	100 cm^{-1}	
Y_2O_3:Eu	32	80	Reflection	0.7	0.33	0.15	Lab. prepared screen
Y_2O_3:Eu	32	80	Transmission	0.69	0.31	0.13	Lab. prepared screen
Gd_2O_2S:Tb[b]	31.7	30	Transmission	0.8	0.38	0.09	Kodak Min-R
Gd_2O_2S:Tb[c]	31.7	30	Reflection	0.78	0.42	0.24	Kodak Min-R
Gd_2O_2S:Tb[d]	31.7	30	Reflection	0.8	0.39	0.16	Kodak Min-R
$YTaO_4$[e]	37.5	70	Transmission	0.75	0.3	0.11	Dupont Ultra-Vision

[a]MTFs were approximately derived from published data.
[b]Nishikawa and Yaffe (Ref. 21).
[c]Van Metter and Rabbani (Ref. 31).
[d]Nishikawa and Yaffe (Ref. 30).
[e]Beutel *et al.* (Ref. 16).

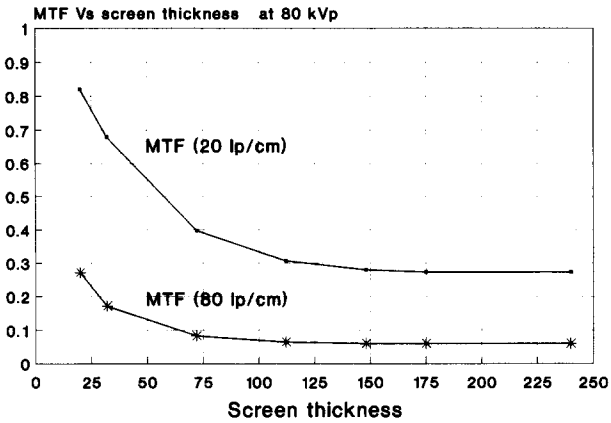

FIG. 9. Variation of Y_2O_3:Eu^{3+} MTFs with screen thickness at 80 lp/cm and at 20 lp/cm.

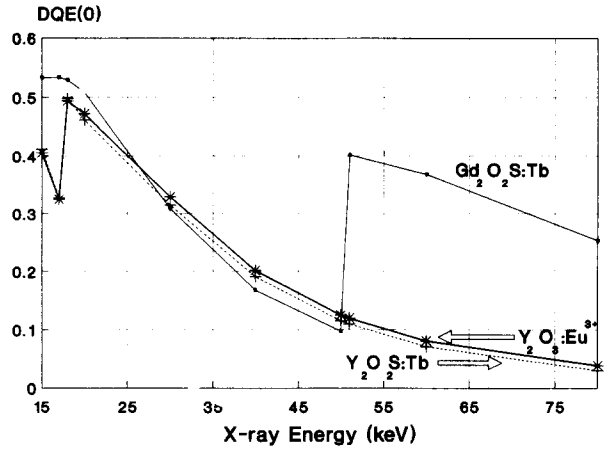

FIG. 11. Variation of DQE(0) with x-ray energy of Gd_2O_2S:Tb, Y_2O_2S:Tb, and Y_2O_3:Eu^{3+} 55 mg/cm^2 screens; curves have been corrected for K fluorescence.

ing DQE at thicker screens. As it can be observed in Fig. 10, DQE starts to degrade for screens thicker than 110 mg/cm^2 at 80 kVp. The effect of x-ray tube voltage on DQE is related to x-ray detection efficiency. For x-ray tube voltages well above the K-absorption edge of yttrium (17 keV), the detection efficiency decreases with increasing voltage, inducing a similar reduction in DQE, as is shown in Fig. 10.

The variation of zero frequency DQE with x-ray energy is shown in Fig. 11 for Y_2O_3:Eu^{3+}, Y_2O_2S:Tb, and Gd_2O_2S:Tb screens of the same thickness. Results were obtained for the three materials under the same conditions and following the same methods. Curves were corrected for the effect of K-fluorescent x rays of yttrium and gadolinium for energies above 17 keV and 50.2 keV, respectively, according to the methods of Chan and Doi[29] and Fahrig *et al.*[23] The DQE of Y_2O_3:Eu^{3+} was found slightly better than that of Y_2O_2S:Tb in the whole energy range and higher than that of Gd_2O_2S:Tb between 30 and 50 keV. This was due to the combined effect of higher σ values for Y_2O_2S:Tb and Gd_2O_2S:Tb and of the lower x-ray absorption efficiency of Gd_2O_2S:Tb in a limited energy range.

Figure 12 shows the measured emission spectrum of Y_2O_3:Eu^{3+} normalized to unity and the normalized spectral sensitivity distribution functions of various commonly employed optical photon detectors; the sensitivity distributions of optical detectors cover a much wider wavelength region than the small portion of interest shown. The Y_2O_3:Eu^{3+} spectrum contains a sharp peak at 613 nm which is in the red color region of the optical spectrum. Photons of such wavelengths undergo less scattering as compared to green light photons emitted by terbium activated phosphors, used in medical imaging (e.g., Gd_2O_2S:Tb, La_2O_2S:Tb, Y_2O_2S:Tb).[25,26] Thus, although terbium activated phosphors have higher values of intrinsic conversion efficiency than Y_2O_3:Eu^{3+}, their corresponding image transfer characteristics are comparable (Table I and Fig. 11). The spectrum of Y_2O_3:Eu^{3+} is narrow enough to assure very good spectral compatibility with the spectral sensitivities of many optical detectors. Table II shows the calculated values of spectral matching factors of Y_2O_3:Eu^{3+} phosphor with various optical detectors. The spectral compatibility with GaAs and S-25 photocathodes, used in photomultiplier and image intensifier

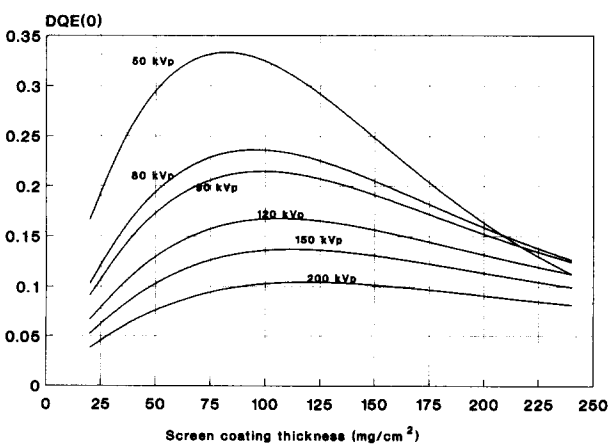

FIG. 10. Variation of the zero frequency DQE of Y_2O_3:Eu^{3+} screens with coating thickness at various x-ray tube voltages.

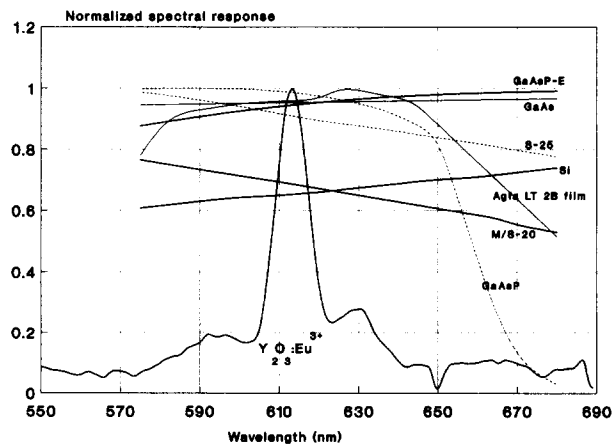

FIG. 12. Normalized spectral response of the Y_2O_3:Eu^{3+} scintillator against normalized spectral sensitivities of various optical detectors.

TABLE II. Matching factor values between the Y_2O_3:Eu^{3+} light spectrum and the spectral sensitivity distributions of various optical detectors.

Optical Detector	Matching Factor
Photocathode GaAs	0.955
Photocathode S-25	0.899
Photocathode modified S-20	0.673
Photocathode extended S-20	0.618
Photodiode Si	0.662
Photodiode Ge	0.353
Photocell GaAsP-E	0.948
Photocell GaAsP	0.895
Agfa Scopix LT 2B film	0.922

tubes, was excellent (matching factor close to or better than 0.9). The same holds for the Agfa Scopix LT 2B film, indicating that this photosensitive emulsion could be used in radiographic applications with Y_2O_3:Eu^{3+} screens. Excellent compatibility was also achieved with GaAsP photocells. Very good compatibility was obtained with an Si photodiode, used in solid state CT detectors and CCD arrays of some digital radiographic systems,[32] and with the modified S-20 photocathode, used in image intensifier and photomultiplier tubes.

IV. SUMMARY AND CONCLUSIONS

The absolute luminescence efficiency, the intrinsic x ray to light conversion efficiency, the light emission spectrum, and optical parameters related to light scattering, absorption, and reflection properties of laboratory prepared Y_2O_3:Eu^{3+} phosphor screens were determined using experimental methods. The optical parameters of the phosphor material were used to calculate the MTF and zero spatial frequency DQE. The spectral compatibility of Y_2O_3:Eu^{3+} to various optical detectors was examined. Coating thicknesses and x-ray tube voltages achieving the best performance of Y_2O_3:Eu^{3+} screens in both transmission and reflection modes of observation, as well as best screen-optical detector combinations were determined. In conclusion, Y_2O_3:Eu^{3+} is a phosphor material displaying satisfactory optical and image transfer properties and could be employed as a radiation detector and medical image receptor.

ACKNOWLEDGMENT

This study is dedicated to the memory of Professor G. E. Giakoumakis, leading member of our team, whose work on phosphor materials has inspired us all to continue.

APPENDIX A: ABSOLUTE EFFICIENCY

The AE was calculated considering a phosphor screen enclosed between two substrates. The absorption of an infinitesimal quantity of x rays dl_x in a thin fluorescent layer dt at depth t is given[9] by

$$dl_x(t) = -\mu(e) l_0 dt \exp(-\mu(e)t), \tag{A1}$$

where $\mu(e)$ is the x-ray mass attenuation coefficient and l_0 is the intensity of x rays at depth $t=0$.

The intensity of light dl_L created within this layer is

$$dl_L(t) = n_c dl_x(t), \tag{A2}$$

where n_c is the intrinsic x ray to light conversion efficiency of the phosphor material. Considering only forward and backward direction of light penetration, dl_L may be divided into two fluxes dl_F and dl_B for forward and backward light propagation. Thus, Eq. (A2) may be equally represented by

$$dl_F(t) = \frac{1}{2} n_c l_0 \mu(e) dt \exp(-\mu(e)t), \tag{A3}$$

$$dl_B(t) = -\frac{1}{2} n_c l_0 \mu(e) dt \exp(-\mu(e)t). \tag{A4}$$

Taking into account light scattering and absorption phenomena during light transmission through the screen material relations (A3) and (A4) may be written as

$$dl_F(t) = \frac{1}{2} n_c l_0 \mu(e) dt \exp(-\mu(e)t) - a l_F(t) dt - s l_F(t) dt + s l_B(t) dt, \tag{A5}$$

$$dl_B(t) = -\frac{1}{2} n_c l_0 \mu(e) dt \exp(-\mu(e)t) + a l_B(t) dt + s l_B(t) dt - s l_F(t) dt. \tag{A6}$$

The first term of both equations describes the x-ray absorption and the light creation efficiency (n_c) of the phosphor material. The second and third terms describe the optical photon loses due to scattering (s) and absorption (a), and the fourth term corresponds to optical photons scattered in a direction opposite to that of light propagation. The second, third, and fourth terms also express the light transmission efficiency of the phosphor material.

For the solution of the differential equations (A5) and (A6) two boundary conditions were considered:

a: at the front screen surface $t=0$:

$$l_F(0) = r_0 l_B(0), \tag{A7}$$

where r_0 is the reflectivity of the front screen-substrate interface.

b: at the back screen surface $t=T$:

$$l_B(T) = r_1 l_F(T), \tag{A8}$$

where r_1 is the reflectivity of the back screen-substrate interface and T is the screen thickness.

Considering that the AE is defined as the ratio of the light flux emitted to the incident x-ray intensity then AE is expressed by

$$n_T(e) = T r_T l_F(T)/l_0, \tag{A9}$$

$$n_R(e) = T r_R l_B(0)/l_0, \tag{A10}$$

where Tr_T,Tr_R are the light transparencies through the two substrates, and $n_T(e)$ and $n_R(e)$ are the monoenergetic absolute efficiencies in transmission and reflection modes of observation, respectively. By solving the differential equations (A5) and (A6), and taking into account relations (A9) and (A10)

$$n_T(e)=\frac{n_c y T_r \mu(1+\rho_1)e^{-\mu T}}{2(\mu^2-\sigma^2)}\,\frac{(\mu-\sigma)(1-\beta)e^{-\sigma T}+2(\sigma+\mu\beta)e^{\mu T}-(\mu+\sigma)(1+\beta)e^{\sigma T}}{(1+\beta)(\rho_1+\beta)e^{\sigma T}-(1-\beta)(\rho_1-\beta)e^{-\sigma T}} \tag{A11}$$

for transmission mode and

$$n_R(e)=\frac{n_c y \mu e^{-\mu T}}{(\mu^2-\sigma^2)}\,\frac{(\mu-\sigma)(\rho_1+\beta)e^{\sigma T}+2(\sigma\rho_1-\mu\beta)e^{-\mu T}-(\mu+\sigma)(\rho_1-\beta)e^{-\sigma T}}{(1+\beta)(\rho_1+\beta)e^{\sigma T}-(1-\beta)(\rho_1-\beta)e^{-\sigma T}} \tag{A12}$$

for reflection mode. n_T,n_R are the absolute efficiencies in transmission and reflection modes, respectively, n_c is the intrinsic x ray to light conversion efficiency of the phosphor, μ is the energy dependent mass attenuation coefficient of the incident x-ray photons, T is the coating thickness (surface density) of the screen, T_r is the transparency of the screen's substrate (Tr=0.9), ρ_1 was calculated by $\rho_1=(1-r_1)/(1+r_1)$, where r_1 is the reflectivity at the screen-substrate interface, y is the conversion factor converting the exposure rate (mR s^{-1}) to energy fluence of the x-ray beam (W m^{-2}), σ and β are coefficients directly related to optical absorption (a) and optical scattering (s) coefficients by $\sigma=[a(a+2s)]^{1/2}$ and $\beta=[a/(a+2s)]^{1/2}$. Experimental data on AE were fitted by Eq. (A13) employing the Levenberg–Marquard method,[33] after determining initial values for n_c from published data on cathodoluminescence measurements, and estimating initial values for σ by inspection.

From hereafter the equations used for the calculation of AE,[9,10,12,34,35] MTF,[12,15,30,31,34] and DQE[15,19,20,21,23,31,34] are presented in discrete form for ease of computer reproduction. The polyenergetic AE of a phosphor screen was calculated by

$$\mathrm{AE}=\frac{\sum_{e=0}^{E_0(\mathrm{kVp})} f(e)n(e)}{\sum_{e=0}^{E_0(\mathrm{kVp})} f(e)}, \tag{A13}$$

where $f(e)$ is the x-ray spectral distribution function given by

$$f(e)=(1-e/E_0)e^{-\mu_{\mathrm{Al}}t_{\mathrm{Al}}}, \tag{A14}$$

where μ_{Al} and t_{Al} are the x-ray mass attenuation coefficient and thickness of the filter material used, respectively. In our experiments the filter material was aluminum with a total thickness of 22 mm (2 mm tube filter+20 mm Al filter for simulating x-ray attenuation by human tissues). The energy step used in (A13) over the whole energy spectrum was 1 keV and E_0 denotes the maximum x-ray spectral energy, numerically equal to the x-ray tube voltage expressed in kVp.

The spectral distribution function $f(e)$ for x rays given by (A14) does not include the K-characteristic radiation emitted by the tungsten target of the x-ray tube. The intensity of this radiation has been described by empirical formulas:[36,37]

$$l_K=C_K(E_0-E_K)^{n_K}, \tag{A15}$$

where E_K is the binding energy of the K shell, C_K,n_K are constants,[36,37] and E_0 is the kinetic energy of the electrons incident on the target. The ratio of the total K-characteristic radiation to the total radiation emitted by a tungsten target has been calculated[36] and experimentally determined.[37] This ratio continuously increases with energy up to 300 kVp. However, if 1 mm Cu filtration is used, ratio maximum (0.095) is reached at 70–80 kVp.[37] The contribution of K-characteristic radiation in our experiments (22 mm Al) was evaluated by employing a formula from a recently published semi-empirical model for generating tungsten x-ray spectra:[38]

$$N(E_i)=A_K\left(\frac{T_0}{E_K}-1\right)^{n_K} f(E_i)\sum_{i=0}^{n} P\left(\frac{x_i}{R}\right) \times\exp[-\mu(E_i)x_i/\sin\theta], \tag{A16}$$

where $x_i=i\Delta x$, $i=0,1,2,\ldots,n$, $R=n\Delta x$, and Δx is the incremental target thickness travelled by the penetrating electrons. A_K,n_K are model parameters, T_0 is the initial energy of the electrons impinging on the target, E_K is the binding energy of the K shell, E_i, is the energy of the characteristic x rays, $f(E_i)$ is the fractional emission of the characteristic x ray of energy E_i, R is the distance at which the average kinetic energy of the electrons becomes equal to E_K,[38] θ=30° is the tube target angle, x is the distance of electron penetration, and $P(x_i/R)$ is a probability distribution function given by

$$P\left(\frac{x_i}{R}\right)=\left(\frac{3}{2}\right)\left[1-\left[\frac{x_i}{R}\right]^2\right] \quad \text{for } x_i\leq R,$$

$$P\left(\frac{x_i}{R}\right)=0 \quad \text{for } x_i>R. \tag{A17}$$

This function accounts for the initial increase in characteristic x-ray production with depth, attributed to the backscattered electrons escaping from the target. After a maximum of characteristic x-ray production is reached, a decrease follows, as the electrons penetrate deeper within the target material.

Values for A_K, n_K, $f(E_i)$, E_i, and E_K were taken from Tucker *et al.*[38] The exposure associated with the characteris-

tic radiation of the target was estimated by taking into account the photon fluence per roentgen.[38] The ratio of the K exposure to the total x-ray exposure was found to be 0.048 at 80 kVp, 0.051 at 90 kVp, 0.067 at 100 kVp, 0.065 at 110 kVp, and 0.061 at 140 kVp, decreasing thereafter. This ratio expresses the extend of the error made in the calculations by employing Eq. (A14). Considering the error involved to be small it was not taken into account in the calculations.

APPENDIX B: MODULATION TRANSFER FUNCTION

The MTF of a phosphor screen of thickness T was calculated considering that it is divided into a number of thin layers of thickness $\Delta t=1$ mg/cm^2. For a thin layer at depth t, a fraction $R_x(e,t)$ of x-ray photons of energy e is absorbed, for each x-ray photon absorbed a number of light photons $m_0(e)$ are created, and a spatial frequency dependent fraction $G(v,t)$ of those light photons is transmitted through the phosphor material and escapes from the screen. Thus, the total number of photons $N(e,v,t)$ emitted from the screen that were generated in a thin layer of thickness $\Delta t=1$ mg/cm^2 at depth t is given by

$$N(e,v,t)=R_x(e,t)m_0(e)G(v,t), \tag{B1}$$

where

$$R_x(e,t)=\mu(e)e^{-\mu(e)t}, \tag{B2}$$

$$m_0(e)=n_c(e/E_P). \tag{B3}$$

E_P is the energy of the optical photons (2.16 eV) and $G(v,t)$ has been derived by Swank[15] by modeling the optical photon propagation through the phosphor material with a diffusion equation whose solution gives

$$G_T(v,t)=\frac{\tau\rho_1[(q+\tau\rho_0)e^{qt}+(q-\tau\rho_0)e^{-qt}]}{(q+\tau\rho_0)(q+\tau\rho_1)e^{qT}-(q-\tau\rho_0)(q-\tau\rho_1)e^{-qT}}, \tag{B4}$$

$$G_R(v,t)=\frac{\tau\rho_1[(q+\tau\rho_0)e^{q(T-t)}+(q-\tau\rho_0)e^{-q(T-t)}]}{(q+\tau\rho_0)(q+\tau\rho_1)e^{qT}-(q-\tau\rho_0)(q-\tau\rho_1)e^{-qT}}, \tag{B5}$$

where $G_T(v,t),G_R(v,t)$ correspond to transmission and reflection mode of measurement, respectively, τ is the inverse relaxation length, q is an optical parameter given by

$$q=[\sigma^2+4\pi^2v^2/d^2]^{1/2}, \tag{B6}$$

where d is the density of the Y_2O_3:Eu^{3+} phosphor coating ($d=1.8$ g/cm^3), measured in powder form, ρ_0,ρ_1 are given by

$$\rho_n=\frac{(1-r_n)}{(1+r_n)} \quad n=0,1, \tag{B7}$$

where r_0,r_1 are the reflectivities at the front screen surface (x-ray incidence side) and the screen-substrate interface respectively. T in (B4) or (B5) is the total screen thickness. The inverse relaxation length τ is related to optical parameters β, σ of relations (A11) and (A12) by $\tau=\sigma/\beta$. $G(v,t)$ divided by $G(0,t)$ gives the MTF of the thin layer Δt at depth t.

The total number of light photons emitted by the screen per x ray absorbed in the phosphor material $G(v,e)$ is calculated by summing the number of photons $N(e,v,t)$ from each layer and dividing by the total fraction of x rays of energy e absorbed in the screen:

$$G(v,e)=\sum_{t=1}^{T}R_x(e,t)m_0(e)G(v,t)\Big/\sum_{t=1}^{T}R_x(e,t). \tag{B8}$$

For a polyenergetic x-ray beam the total number of photons emitted per absorbed x ray is calculated by averaging over the x-ray spectrum $f(e)$

$$G(v)=\sum_{e=1}^{E_0}f(e)G(v,e)\Big/\sum_{e=1}^{E_0}f(e), \tag{B9}$$

where E_0 is the x-ray tube voltage. The MTF was then calculated by normalizing (B9) to unity at zero frequency:

$$\mathrm{MTF}(v)=G(v)/G(0). \tag{B10}$$

APPENDIX C: ZERO SPATIAL FREQUENCY DETECTIVE QUANTUM EFFICIENCY

The information content of a medical image may be quantitatively expressed by the signal to noise ratio (SNR). The efficiency of a screen to transfer information may be expressed by the information content reaching the output of the screen compared to the information content at the screen input. This may be evaluated by means of the DQE, which relates the output SNR to the input SNR:

$$\mathrm{DQE}=\left[\frac{\mathrm{SNR_{out}}}{\mathrm{SNR_{in}}}\right]^2. \tag{C1}$$

It has been shown[19,20] that DQE may be equivalently expressed by

$$\mathrm{DQE}=A_QA_S, \tag{C2}$$

where A_Q is the quantum detection efficiency, which expresses the fraction of incident x rays that are absorbed in the screen material. A_Q was calculated by

$$A_Q=\sum_{e=1}^{E_0}f(e)[1-e^{-\mu(e)T}]\Big/\sum_{e=1}^{E_0}f(e). \tag{C3}$$

A_S is the Swank factor (or statistical factor) that describes the fluctuation in the number of optical photons emitted per absorbed x ray. These fluctuations result in a statistical optical pulse height distribution characterized by its statistical moments. A_S is defined as

$$A_S=M_1^2/M_0M_2, \tag{C4}$$

where M_i, $i=0,1,2$ are the zeroth, first, and second statistical moments of the optical pulse (scintillation) height distribution. The polyenergetic moments of the optical pulse height distribution, necessary for the calculation of the Swank factor, were determined by the equations:

$$M_0=1, \tag{C5}$$

$$M_1=\sum_{e=1}^{E_0} f(e)M_1(e) \Big/ \sum_{e=1}^{E_0} f(e), \quad \text{(C6)}$$

where

$$M_1(e)=\sum_{t=1}^{T} m_0(e)G(0,t)R_x(e,t) \Big/ \sum_{t=1}^{T} R_x(e,t) \quad \text{(C7)}$$

is the monoenergetic first moment and $R_x(e,t)$ is given in (B2) and $G(0,t)$ in (B4) and (B5). The product $m_0(e)G(0,t)$ expresses the number of emitted optical photons per x-ray absorbed originating from a thin layer at depth t.

$$M_2=\sum_{e=1}^{E_0} f(e)M_2(e) \Big/ \sum_{e=1}^{E_0} f(e), \quad \text{(C8)}$$

and

$$M_2(e)=\sum_{t=1}^{T} m_0^2(e)G^2(0,t)R_x(e,t) \Big/ \sum_{t=1}^{T} R_x(e,t), \quad \text{(C9)}$$

where $M_2(e)$ is the monoenergetic second moment.

[a]Please address correspondence: Prof. D. Cavouras, Ph.D., Dept. of Medical Instrumentation Technology, 37-39 Esperidon Street, Kallithea 17671, Athens, Greece, Tel: (+301) 9594-558, Fax: (+301) 9594-558, (+301) 5910 975, Electronic mail: cavouras@hol.gr, cavouras@ee.teiath.gr.

[1]S. Tanaka, Y. Maruyama, H. Kobayashi, and H. Sasakura, "Electroluminescence in rare earth doped Y_2O_3,La_2O_3, and Y_2O_2S powder layers," J. Electrochem. Soc. **123**, 1917–1918 (1976).

[2]B. Zurro, A. Ibarra, K. J. McCarthy, A. U. Acuna, and R. Sastre, "Comparison of phosphors for broadband plasma emission detectors," Rev. Sci. Instrum. **66**, 534–536 (1995).

[3]T. S. Curry, J. E. Dowdey, and R. C. Murry, *Christensen's Physics of Diagnostic Radiology*, 4th ed. (Lea & Febiger, Philadelphia, 1990), pp. 127, 172.

[4]*Lumilux Data Book* (Riedel-deHaen, Seelze, Germany, 1989).

[5]B. A. Arnold, "Physical characteristics of screen-film combinations," in *The Physics of Medical Imaging: Recording System, Measurements and Techniques*, edited by A. G. Haus (American Association of Physicists in Medicine, New York, 1979), pp. 30–71.

[6]D. R. Morgan, R. A. Sones, and G. T. Barnes, "Performance characteristics of dual-energy detector for digital scan projection radiography," Med. Phys. **14**, 728–735 (1987).

[7]R. C. Alig and S. Bloom, "Cathodoluminescent efficiency," J. Electrochem. Soc. **124**, 1136–1138 (1977).

[8]G. Zweig and D. A. Zweig, "Radioluminescent imaging: Factors affecting total light output," Proc. SPIE **419**, 297–304 (1983).

[9]G. W. Ludwig, "X-ray efficiency of powder phosphors," J. Electrochem. Soc. **118**, 1152–1159 (1971).

[10]G. E. Giakoumakis, C. D. Nomicos, P. Skountzos, S. Koutroubas, A. Zisos, E. N. Yiakoumakis, M. C. Katsarioti, J. A. Kaliakatsos, M. Rovithi, G. S. Panayiotakis, and E. K. Evangelou, "Y_2O_2S:Eu phosphor screens evaluation," Med. Phys. **20**, 79–83 (1993).

[11]G. E. Giakoumakis, "Matching factors for various light-source-photodetector combinations," Appl. Phys. A **52**, 7–9 (1991).

[12]H. Hamaker, "Radiation and heat conduction in light-scattering material," Phili. Res. Rep. **2**, 55–67 (1947).

[13]E. Storm and H. Israel, "Photon cross-sections from 0.001 to 100 MeV for elements 1 through 100," Report LA-3753, Los Alamos Scientific Laboratory of the University of California (1967).

[14]E. B. Saloman, J. H. Hubbell, and J. H. Scofield, "X-ray attenuation cross-sections for energies 100 eV to 100 keV and elements $Z=1$ to $Z=92$," At. Data Nucl. Data Tables **38**, 1–197 (1988).

[15]R. K. Swank, "Calculation of modulation transfer functions of x-ray fluorescent screens," Appl. Opt. **12**, 1865–1870 (1973).

[16]J. Beutel, B. A. Apple, and R. Shaw, "The role of screen parameters and print-through in the performance of film/screen systems," Phys. Med. Biol. **38**, 1181–1193 (1993).

[17]G. T. Barnes, "The use of bar pattern test objects in assessing the resolution of film/screen systems," in *The Physics of Medical Imaging Recording System Measurements and Techniques*, edited by A. G. Haus (American Association of Physicists in Medicine, New York, 1979), pp. 138–151.

[18]W. Hillen, U. Schiebel, and T. Zaengel, "Imaging performance of a digital storage phosphor system," Med. Phys. **14**, 744–751 (1987).

[19]R. K. Swank, "Absorption and noise in x-ray phosphors," J. Appl. Phys. **44**, 4199–4203 (1974).

[20]C. E. Dick and J. W. Motz, "Image information transfer properties of x-ray fluorescent screens," Med. Phys. **8**, 337–346 (1981).

[21]R. M. Nishikawa and M. J. Yaffe, "Model of the spatial-frequency-dependent detective quantum efficiency of phosphor screens," Med. Phys. **17**, 894–904 (1990).

[22]A. Ginzburg and C. E. Dick, "Image information transfer properties of x-ray intensifying screens in the energy range from 17 to 320 keV," Med. Phys. **20**, 1013–1021 (1993).

[23]R. Fahrig, J. A. Rowlands, and M. J. Yaffe, "X-ray imaging with amorphous selenium: Detective quantum efficiency of photoconductive receptors for digital mammography," Med. Phys. **22**, 153–160 (1995).

[24]P. Haque and J. H. Stanley, "Basic principles of computed tomography detectors," in *Radiology of the Skull and Brain: Technical Aspects of Computed Tomography*, edited by T. H. Newton and D. G. Potts (C. V. Mosby, St. Louis, MO, 1981), p. 4103.

[25]G. E. Giakoumakis, C. D. Nomicos, E. N. Yiakoumakis and E. K. Evangelou, "Absolute efficiency of rare earth oxysulfide screens in reflection mode observation," Phys. Med. Biol. **35**, 1017–1023 (1990).

[26]I. Kandarakis, D. Cavouras, G. Panayiotakis, T. Agelis, C. Nomicos, and G. Giakoumakis, "X-ray induced luminescence and spatial resolution of La_2O_2S:Tb phosphor screens," Phys. Med. Biol. **41**, 297–307 (1996).

[27]B. A. Arnold and B. E. Bjorngard, "The effect of phosphor K x-rays on the MTF of rare-earth screens," Med. Phys. **6**, 500–503 (1979).

[28]W. Que and J. A. Rowlands, "X-ray imaging using amorphous selenium: Inherent spatial resolution," Med. Phys. **22**, 365–374 (1995).

[29]H. P. Chan and K. Doi, "Energy and angular dependence of x-ray absorption and its effect on radiographic response in screen-film systems," Phys. Med. Biol. **28**, 565–579 (1983).

[30]R. M. Nishikawa and M. J. Yaffe, "Modeling of the spatial-frequency-dependent detective quantum efficiency of x-ray image receptors," SPIE **914**, 128–138 (1988).

[31]R. Van Metter and M. Rabbani, "An application of multivariate moment-generating functions to the analysis of signal and noise propagation in radiographic screen-film systems," Med. Phys. **17**, 65–71 (1990).

[32]A. D. Maidment and M. J. Yaffe, "Analysis of signal propagation in optically coupled detectors for digital mammography: I. Phosphor screens," Phys. Med. Biol. **40**, 877–889 (1995).

[33]W. H. Press, B. P. Flannery, S. A. Teukolsky, and W. T. Vetterling, *Numerical Recipes in Pascal: The Art of Scientific Computing* (Cambridge U. P., Cambridge, 1989), pp. 575–580.

[34]E. Storm, "Calculated bremsstrahlung spectra from thick tungsten targets," Phys. Rev. A **5**, 2328–2338 (1972).

[35]W. R. Hendee, *Medical Radiation Physics* (Year Book Medical Publishers, Chicago, 1970), pp. 145–148.

[36]E. Storm, "Emission of characteristic L and K radiation from thick tungsten targets," J. Appl. Phys. **43**, 2790–2796 (1972).

[37]P. Tothill, "The ratio of K characteristics to the total radiation emitted from a tungsten target X-ray tube," Brit. J. Appl. Phys. (J. Phys. D) **1**, 1093–1107 (1968).

[38]D. M. Tucker, G. T. Barnes, and D. P. Chakraborty, "Semi-empirical model for generating tungsten target x-ray spectra," Med. Phys. **18**, 211–218 (1991).